Materials Research. 2021; 24(1): e20200366
DOI: https://doi.org/10.1590/1980-5373-MR-2020-0366

Synthesis of the $La_3Ba_5Cu_8O_{18-\delta}$ and $Sm_3Ba_5Cu_8O_{18-\delta}$ superconductors by the combustion and solid-state reaction methods

U. Fuentes Guerrero[a*], *A.M. Morales Rivera*[a], *J.A. Gómez Cuaspud*[a], *J. Munevar*[b], *C.A. Parra Vargas*[a]

[a]*Universidad Pedagógica y Tecnológica de Colombia, Grupo Física de Materiales, Avenida Central del Norte 39-115 Tunja, Boyacá, Colombia*
[b]*Universidade Federal do ABC (UFABC), CCNH, SP 09210-580, Santo André, SP, Brasil*

Received: August 13, 2020; Revised: November 04, 2020; Accepted: November 29, 2020.

In this paper, the synthesis of the $La_3Ba_5Cu_8O_{18-\delta}$ and $Sm_3Ba_5Cu_8O_{18-\delta}$ superconductors using the combustion method is reported for the first time. Besides, a comparison with the solid-state reaction method was performed. The materials were synthesized at 870 °C for 24 h under oxygen flow. Rietveld refinement showed materials with the main crystal phase corresponding to the orthorhombic structure of space-group *Pmm2* (25), with purity in the range 51-85%, which had not reported for the RE358 systems. On the other hand, the magnetic measurements under external fields (30 and 100 Oe) confirmed the diamagnetic response associated with the Meissner effect, and T_c values between 24 and 58 K.

Keywords: *Superconductor, combustion, solid-state reaction.*

1. Introduction

The YBCO family of superconductors is constituted by the materials $YBa_2Cu_3O_{7-\delta}$ (Y123) with a critical temperature (T_c) of 90 K[1,2], $YBa_2Cu_4O_8$ (Y124), $Y_2Ba_4Cu_7O_{15}$ (Y247) and $Y_3Ba_5Cu_8O_{18}$ (Y358), which differ on the number of CuO_2 planes and CuO chains[3]. These superconductors have electronic and magnetic applications, such as electric motors, particle accelerators, magnetic levitation devices, and cables[4].

Y358 superconductor exhibits the highest T_c (98 K), it has an orthorhombic structure of space-group *Pmm2* (25) and its unit cell is similar to that of Y123, with *a* and *b* parameters very similar. Nevertheless, the *c* parameter is almost three times larger than the one of Y123[5]. Y123 superconductor is constituted by two CuO_2 planes and a CuO chain, Y124 by a double CuO chain, while Y247 has a CuO_2 plane and a double CuO chain. The Y358 superconductor is similar to Y123, although has five CuO_2 planes and three CuO chains per unit cell. CuO_2 planes are important for the transfer of charge carriers and CuO chains perform as a charge reservoir by not being superconductors[6]. The greater number of planes and chains in the Y358 system generates an increase in the T_c due to a greater amount of electron pairs[7,8].

The RE358 (RE = rare earth) superconductor system has been commonly synthesized by the solid-state reaction method, starting from stoichiometric mixtures of oxides and carbonates, and using high temperatures for a long time[9,10]. This led to the use of wet methods such as sol-gel[11] and combustion[12], which favor obtaining pure materials and nanocrystalline powders[13,14]. Nevertheless, the sol-gel method has disadvantages associated with parameters, which must be carefully modified such as precursors, solvent, and pH, to reach the desired composition, and microstructure properties. An alternative to the sol-gel method is the combustion method among the wet methods due to its simplicity, speed and effectiveness for the synthesis of powders with great homogeneity and nanometric size[15]. Obtaining pure phase materials has not been reported up to now, and the percentage of superconducting phase has not exceeded 73%. Therefore, research to increase this percentage is still carrying out[14,16].

Recent research reported the synthesis of the $Sm_3Ba_5Cu_8O_{18}$ and $Nd_3Ba_5Cu_8O_{18}$ materials through the solid-state reaction method at 950 °C for 60 h, reaching T_c values between 71 and 91 K[17]. $RE_3Ba_5Cu_8O_y$ (RE = Y, Nd, Sm, Gd) materials were obtained at 915 °C for 24 h[18], and $RE_3Ba_5Cu_8O_{18}$ (RE = Sm, Eu, Gd, Dy and Ho) at 880 °C for 48 h, exhibited T_c values in the range 60-85 K[16]. There are no reports about the synthesis of the Sm358 and La358 materials using the combustion method. However, this method been used for the synthesis of superconductor-type $REBa_2Cu_3O_{7-X}$ (RE = Y, Er, Sm and Nd) at 900 °C for 4 h[15] and $LaBa_2Cu_3O_7$ at 800 °C for 2 h under O_2 atmosphere, the previous reports showed that the combustion method allowed the obtaining of highly homogeneous nanomaterials[19]. This research reports the $La_3Ba_5Cu_8O_{18-\delta}$ and $Sm_3Ba_5Cu_8O_{18-\delta}$ superconducting materials synthesized by the combustion method. A comparison between the solid-state reaction and combustion methods was made, evaluating the magnetic and structural properties by X-ray diffraction and magnetization as a function of temperature.

2. Experimental

$Sm_3Ba_5Cu_8O_{18-\delta}$ (Sm358) and $La_3Ba_5Cu_8O_{18-\delta}$ (La358) samples were produced through the combustion and solid-state reaction methods. The samples were obtained for the

*e-mail: ubefuentes@yahoo.es

first time by the combustion method, from 1.0 M solutions of $La(NO_3)_3$, $Ba(NO_3)_2$ and $Cu(NO_3)_2$, to which citric acid was added with a ratio of 1:0.5 regard the concentration of the cations. The resulting solutions were heated at 300 °C until obtaining a solid carbonaceous, and subsequently calcined at 870 °C for 2 h to remove the carbonaceous remnants. Finally, the obtained samples were ground, pressed into pellets under a pressure of 2.5 MPa and sintered at 870 °C, for 24 h under an O_2 flow.

Samples with the same composition were also obtained by the solid-state reaction method, from stoichiometric amounts of samarium (III) oxide (Sm_2O_3-99.999%), lanthanum (III) oxide (La_2O_3-99.999%), copper oxide (II) (CuO-99.999%) and barium carbonate ($BaCO_3$- 99.99%). The oxide powders were ground and decarbonated at 800 °C for 24 h. Afterward, the obtained powders were ground, pressed into pellets under a pressure of 2.5 MPa, and sintered at 870 °C, for 24 h and under O_2 flow.

The structural characterization was performed by X-ray diffraction (XRD) in a PANalytical X'Pert PRO-MPD equipment, using CoKα_1 radiation (λ = 1.7890 Å), from 20 to 90° with a step size of 0.013°, the acquisition time of 99.019 seconds and operating at 40 mA and 40 kV. The XRD patterns were refined by Rietveld method using the GSAS and PCW software suites[20,21]. The magnetization measurements were carried out in a Quantum Design MPMS3 SQUID-VSM magnetometer, with temperatures from 10 to 200 K, under an external applied field of 30 and 100 Oe, respectively.

3. Results and Discussion

The XRD patterns of Sm358 and La358 powdered samples, obtained by solid-state reaction (a) and combustion method (b) are shown in the Figure 1. The XRD patterns of the samples were similar, with a slight shift of peaks towards higher 2θ angles (right panel of Figure 1). This is attributed to the distortion of the unit cell generated by the difference between the ionic radius of Sm^{3+} (1.04 Å) and La^{3+} (1.16 Å), the main XRD peak shifted from 38,01° 2θ (La358) to 38,33° 2θ (Sm358) for the samples obtained by the combustion method, and from 38,00° 2θ (La358) to 38,28° 2θ (Sm358) for those obtained by the solid-state reaction method. The difference of the ionic radii also influenced the crystallite size, which was determined using the Scherrer equation with a constant value of 0.9. The calculated crystallite sizes were: Sm358 = 64 nm and La358 = 79 nm for the combustion method, and Sm358 = 44 nm and La358 = 93 nm for the solid-state reaction method.

The refined diffractograms are shown in Figure 2, where the experimental diffractogram is identified with the symbol (x), the red line corresponds to the refined theoretical model, the blue line is the difference between the theoretical and experimental diffractograms, and the Bragg positions of the identified phases are shown in bars. It was possible to identify a main crystal phase corresponding to $RE_3Ba_5Cu_8O_{18-\delta}$ (RE358), with orthorhombic structure and space-group *Pmm2* (25). The secondary crystal phases were

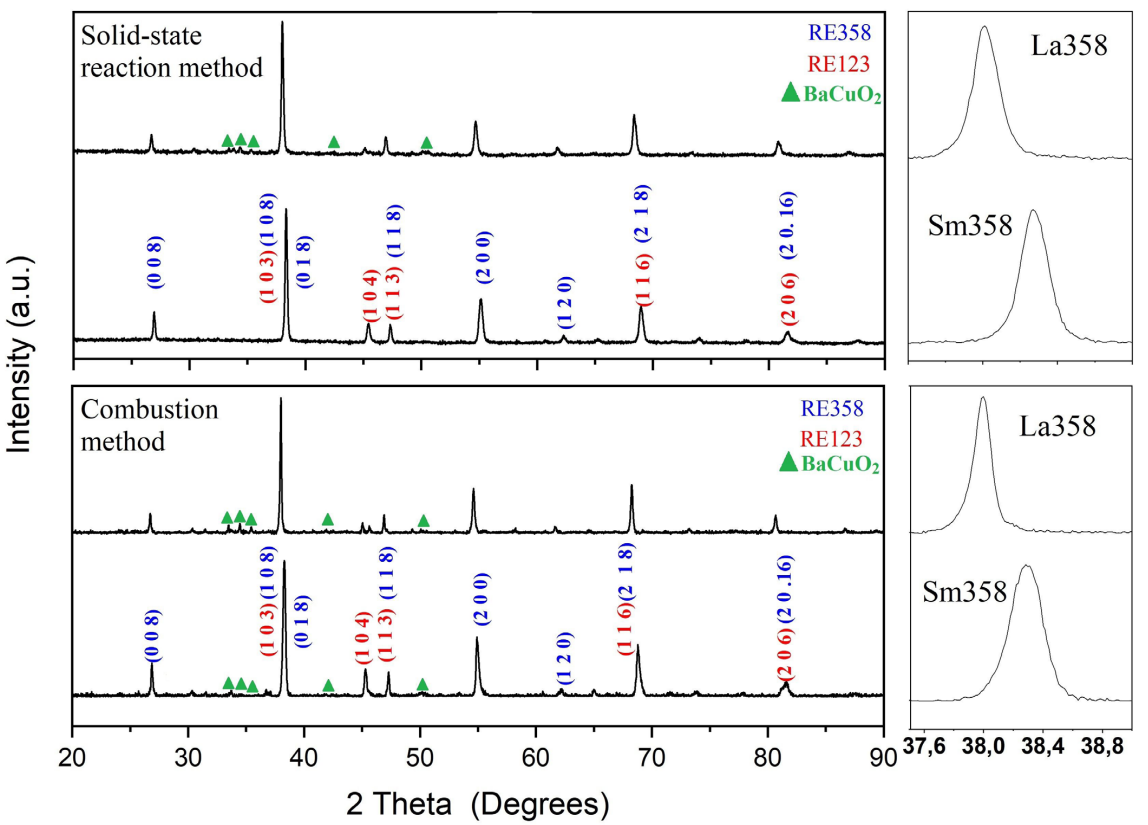

Figure 1. XRD pattern of the $Sm_3Ba_5Cu_8O_{18-\delta}$ and $La_3Ba_5Cu_8O_{18-\delta}$ samples obtained by solid-state reaction and combustion method. Right panel: magnified XRD patterns in the 2θ range 37–39°.

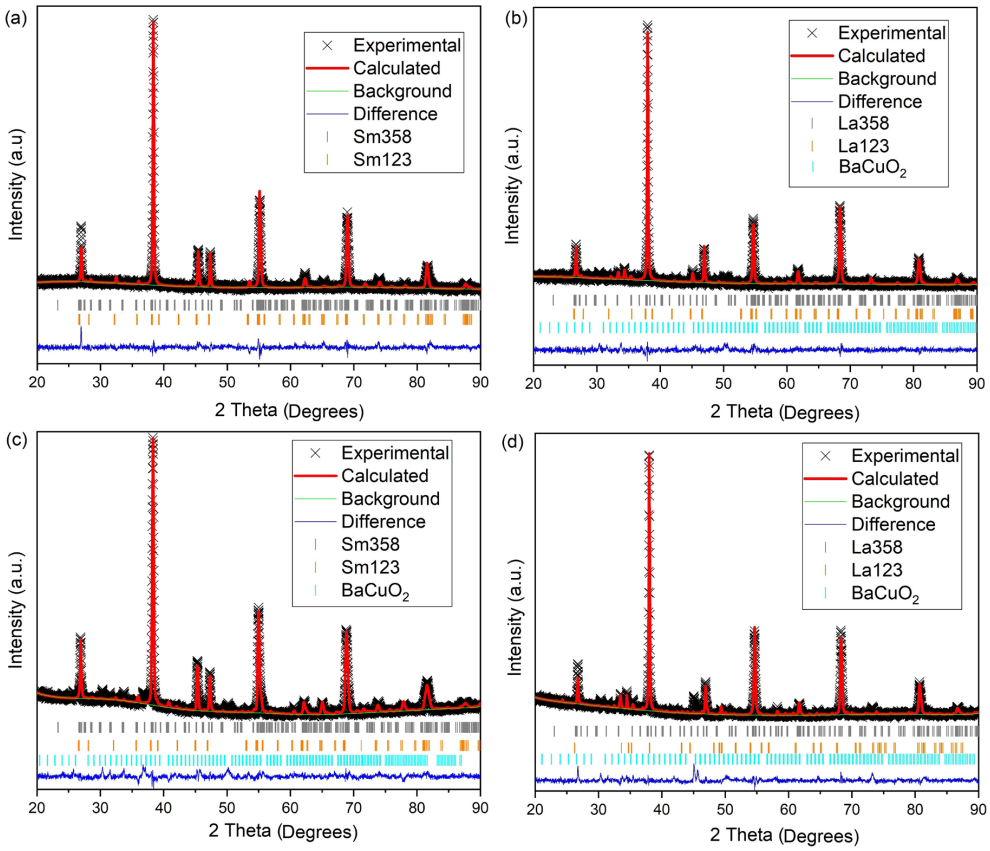

Figure 2. Refined XRD patterns for the $Sm_3Ba_5Cu_8O_{18-\delta}$ and $La_3Ba_5Cu_8O_{18-\delta}$ obtained by combustion (a, b) and solid-state reaction (c, d).

identified, $REBa_2Cu_3O_{6.4}$ (RE123), reported by other authors as the non-superconducting phase, with tetragonal structure of space group *P4/mmm* (123)[7,16], and $BaCuO_2$ with cubic crystal structure of space- group *Im-3m* (229).

Synthesis of the La358 superconductor had not been reported. This can be attributed to that lanthanum is the rare-earth element with the largest ionic radius, hindering the stabilization of the La358 structure, which also explains the presence of more stable secondary phases such as La123 and $BaCuO_2$ in the obtained samples (see Table 1). The XRD peaks in the 2θ range 33 - 36° with the (5 3 0), (4 4 2), and (5 3 2) planes correspond to the $BaCuO_2$ crystal phase, generated by the slow decomposition reaction[22,23]. However, La358 sample was obtained with purities of 50.81% and 85.35% by the method of combustion and solid-state reaction, respectively. Besides, the material purity was advantaged by the high purity and small size of the oxides used in the synthesis.

The atomic positions and occupation factors for the new La358 material are listed in Table 2. The data obtained is in accordance with the previously reported for RE358 systems[11]. Figure 3 shows the crystal structure obtained for the La358 sample, which exhibits the presence of five CuO_2 planes and three CuO chains.

The Sm358 sample obtained for the first time by the combustion method exhibited a purity of 81%, which is higher than those reported up to now[16]. The use of citric acid as a chelating agent favors the homogeneous mixture of the precursors, avoiding the segregation processes and reducing the presence of unwanted crystalline phases.

Figure 4 shows the magnetization as a function of temperature for the obtained samples, the results confirm for the first time a superconducting transition in the new La358 material. T_c values were determined from the cut-off point in the extrapolated lines. The irreversibility temperature (T_{irr}) was determined as the bifurcation point between the ZFC and FC curves (see Figure 4d). Below the T_c, a characteristic diamagnetic contribution of the Meissner effect in the superconducting state was observed. Besides, T_c increased by using a higher magnetic field (see Table 3), which is attributed to T_c does not decrease with magnetic fields below the critical field of the superconductor. The T_{irr} values were lower than T_c, such as has been reported by other authors[24]. The magnetic behavior of the RE123 and $BaCuO_2$ materials has been previously analyzed[16,25], demonstrating that these phases do not affect the superconducting response in the RE358 system.

The difference in ionic radius of La^{3+} and Sm^{3+} modified the distance between superconducting planes, affecting the internal charge transfer from the CuO_2 planes to the charge reservoirs, which generates a decrease in T_c for the La358 sample (see Table 3)[26]. La358 superconductor exhibited larger lattice parameters, which led to a larger cell volume (see Table 1). The increase in the *c* parameter confirms that the distance between the CuO chains is affected

Table 1. Lattice parameters and calculated orthorhombicity (*r*) of the simples by each method.

Method	Sample	χ2	Rf (%)	Phase	Phase proportion (%)	a (Å)	b (Å)	c (Å)	V (Å3)	r
Combustion	Sm358	1.249	0.109	Sm358	81.18	3.896(2)	3.876(7)	31.106(1)	469.8(2)	0.2509
				Sm123	18.82	3.874(2)	3.874(2)	11.666(4)	175.1(2)	
	La358	1.099	0.248	La358	50.81	3.918(2)	3.905(3)	31.293(8)	478.8(5)	0.1674
				La123	38.64	3.921(5)	3.921(5)	11.730(2)	180.3(7)	
				BaCuO2	10.54	18.318(8)	18.318(8)	18.318(8)	6147.3(6)	
Solid-state reaction	Sm358	1.753	0.1407	Sm358	65.59	3.895(1)	3.865(8)	31.093(5)	468.2(3)	0.3775
				Sm123	34.29	3.894(9)	3.894(9)	11.717(4)	177.7(5)	
				BaCuO2	0.12	20.264(9)	20.264(9)	20.264(9)	8322.8(1)	
	La358	1.835	0.2244	La358	85.35	3.906(3)	3.913(4)	31.374(5)	479.6(1)	0.0908
				La123	0.40	3.098(8)	3.098(8)	11.832(4)	113.6(3)	
				BaCuO2	14.25	18.300(1)	18.300(7)	18.300(1)	6128.4(9)	

Table 2. Structural data from Rietveld refinement for the $La_3Ba_5Cu_8O_{18-\delta}$ sample.

Atom	x	y	z	Occ	*U*
La(1)	0.5000	0.5000	1.0000	0.9900	0.025
Cu(1)	0.0000	0.0000	0.0625	1.0000	0.025
O(1)	0.0000	0.5000	0.0625	1.0000	0.025
O(2)	0.5000	0.0000	0.0625	1.0000	0.025
Ba(1)	0.5000	0.5000	0.1250	0.9900	0.025
O(3)	0.0000	0.0000	0.1250	1.0000	0.025
Cu(2)	0.0000	0.0000	0.1875	1.0000	0.025
O(4)	0.0000	0.5000	0.1875	0.9800	0.025
Ba(2)	0.5000	0.5000	0.2500	0.9900	0.025
O(5)	0.0000	0.0000	0.2500	0.9900	0.025
Cu(3)	0.0000	0.0000	0.3125	1.0000	0.025
O(6)	0.0000	0.5000	0.3125	0.9900	0.025
O(7)	0.5000	0.0000	0.3125	1.0000	0.025
La(2)	0.5000	0.5000	0.3750	1.0000	0.025
Cu(4)	0.0000	0.0000	0.4375	1.0000	0.025
O(8)	0.0000	0.5000	0.4375	0.9900	0.025
O(9)	0.5000	0.0000	0.4375	1.0000	0.025
La(3)	0.5000	0.5000	0.5000	1.0000	0.025
Cu(5)	0.0000	0.0000	0.5625	1.0000	0.025
O(10)	0.0000	0.5000	0.5625	1.0000	0.025
O(11)	0.5000	0.0000	0.5625	1.0000	0.025
Ba(3)	0.5000	0.5000	0.6250	0.9900	0.025
O(12)	0.0000	0.0000	0.6250	1.0000	0.025
Cu(6)	0.0000	0.0000	0.6875	1.0000	0.025
O(13)	0.0000	0.5000	0.6875	1.0000	0.025
Ba(4)	0.5000	0.5000	0.7500	0.9900	0.025
O(14)	0.0000	0.0000	0.7500	1.0000	0.025
Cu(7)	0.0000	0.0000	0.8125	1.0000	0.025
O(15)	0.0000	0.5000	0.8125	1.0000	0.025
Ba(5)	0.5000	0.5000	0.8750	0.9900	0.025
O(16)	0.0000	0.0000	0.8750	0.9900	0.025
O(17)	0.0000	0.5000	0.9375	0.9800	0.025
O(18)	0.5000	0.0000	0.9375	0.9900	0.025
Cu(8)	0.0000	0.0000	0.9375	1.0000	0.025

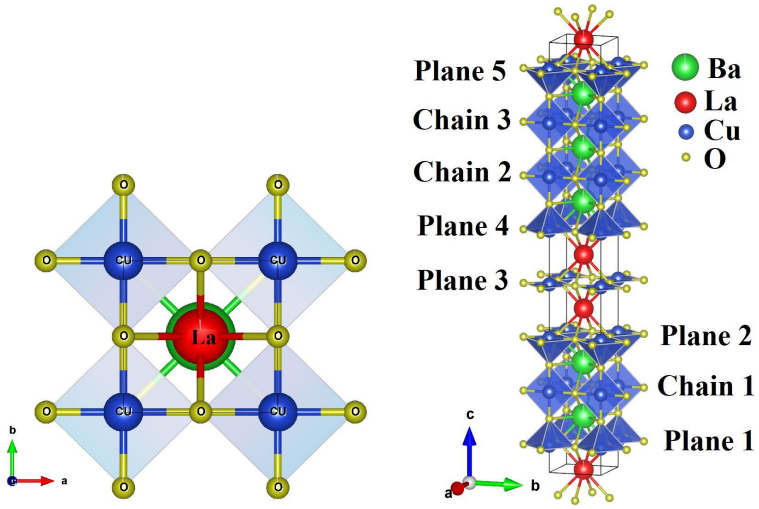

Figure 3. Crystal structure of the $La_3Ba_5Cu_8O_{18-\delta}$ sample obtained by combustion method.

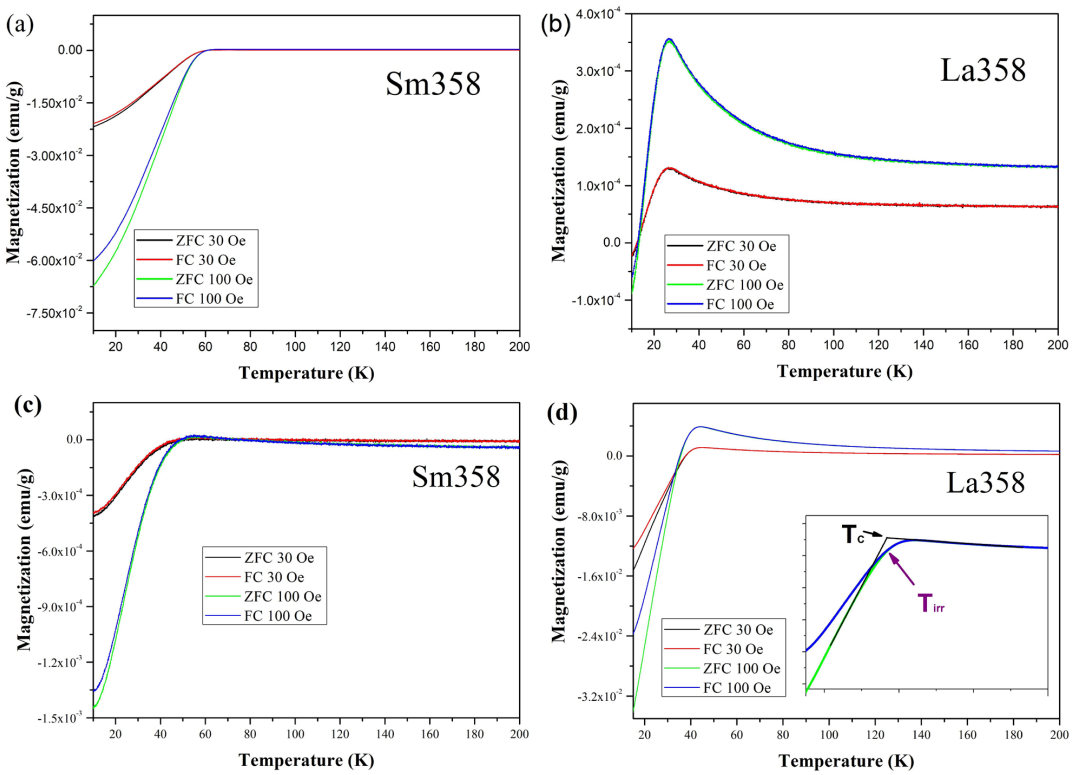

Figure 4. Magnetization as a function of temperature for the $Sm_3Ba_5Cu_8O_{18-\delta}$ and $La_3Ba_5Cu_8O_{18-\delta}$ samples obtained by (a, b) combustion and (c, d) solid-state reaction.

Table 3. T_c and T_{irr} for the $Sm_3Ba_5Cu_8O_{18-\delta}$ and $La_3Ba_5Cu_8O_{18-\delta}$ samples.

Method	H(Oe)	$Sm_3Ba_5Cu_8O_{18-\delta}$		$La_3Ba_5Cu_8O_{18-\delta}$	
		T_c (K)	T_{irr} (K)	T_c (K)	T_{irr} (K)
Solid-state reaction	30	43.30	31.99	39.73	38.03
	100	49.08	44.11	40.57	37.98
Combustion	30	56.59	43.15	23.99	14.41
	100	58.26	49.88	25.59	17.19

by the ionic radius (Sm^{3+} = 1.04 Å and La^{3+} = 1.16 Å), such as was previously reported[4,27].

Orthorhombicity was determined using the equation, r = 100 (*b* - *a*) / (*b* + *a*). La358 superconductor shows a lower orthorhombicity value due to the La^{3+} cations generate a decrease of oxygen concentration in the O(1) site, located in the basal plane along axis b[14,28]. The samples with greater superconducting phase showed a higher T_c, which was influenced by the synthesis method used and the synthesis conditions. Besides, superconductors of higher purity than those reported by other authors were obtained[6,12,14].

4. Conclusion

The $Sm_3Ba_5Cu_8O_{18-\delta}$ and $La_3Ba_5Cu_8O_{18-\delta}$ superconductors were synthesized for the first time using the combustion method, using temperature and time lower than those reported by other authors. The samples obtained by the solid-state reaction and combustion methods, showed a main crystal phase corresponding to RE358 superconductor with an orthorhombic structure of space-group *Pmm2* (25) and crystallite sizes between 44 nm and 93 nm. Magnetic analyzes allowed determining the T_c and T_{irr} values under low applied fields. The results showed that T_c decreased with the increase in the ionic radius of the rare-earth, and increased with the percentage of the superconducting phase.

5. Acknowledgement

The authors thank the Multiuser Central Facilities (CEM-UFABC) for providing access and support to their experimental facilities.

6. References

1. Kordas G, Wu K, Brahme U, Friedmann T, Ginsberg D. High-temperature ceramic superconductors derived from the sol-gel process. Mater Lett. 1987;5(11-12):417-9.
2. Shi D. High-temperature superconducting materials science and engineering: new concepts and technology. Pergamon; 1995.
3. Hashi K, Ohki S, Matsumoto S, Nishijima G, Goto A, Deguchi K, et al. Achievement of 1020 MHz NMR. J Magn Reson. 2015;256:30-3.
4. Dihom MM, Shaari AH, Baqiah H, Kien CS, Azis RS, Abd-Shukor R, et al. Calcium-Substituted $Y_3Ba_5Cu_8O_{18}$ Ceramics Synthesized via Thermal Treatment Method: Structural and Superconducting Properties. J Supercond Nov Magn. 2018;32(7):1875-83.
5. Aliabadi A, Farshchi YA, Akhavan M. A new Y-based HTSC with Tc above 100K. Physica C: Superconductivity and its Applications. 2009;469(22):2012-4.
6. Téllez DA, Báez MC, Roa-Rojas J. Structure and conductivity fluctuations of the $Y_3Ba_5Cu_8O_{18}$ superconductor. Mod Phys Lett B. 2012;26:1-11.
7. Pimentel JL, Buitrago DM, Supelano I, Vargas CAP, Mesquita FR, Pureur P. Synthesis and characterization of the superconductors $Y_3Ba_5Cu_{8-x}Fe_xO_{18}$ ($0.0597 \leq x \leq 0.1255$). J Supercond Nov Magn. 2014;28(2):509-12.
8. Barrera EW, Téllez DA, Roa-Rojas J. Crystallographic analysis and conductivity fluctuations of the $Y_2Ba_5Cu_8O_{17}$ superconductor. Mod Phys Lett B. 2015;29(04):1-8.
9. Slimani Y, Hannachi E, Azzouz FB, Salem MB. Impact of planetary ball milling parameters on the microstructure and pinning properties of polycrystalline superconductor $Y_3Ba_5Cu_8O_y$. Cryogenics. 2018;92:5-12.
10. Topal U, Akdogan M, Ozkan H. Electrical and structural properties of $RE_3Ba_5Cu_8O_{18}$ (RE=Y, Sm and Nd) superconductors. J Supercond Nov Magn. 2011;24(7):2099-102.
11. Gholipour S, Daadmehr V, Rezakhani AT, Khosroabadi H, Shahbaz Tehrani F, Hosseini Akbarnejad R. Structural phase of Y358 superconductor comparison with Y123. J Supercond Nov Magn. 2012;25(7):2253-8.
12. Suan MSM, Johan MR, Siang TC. Synthesis of $Y_3Ba_5Cu_8O_{18}$ superconductor powder by auto-combustion reaction: effects of citrate–nitrate ratio. Physica C. 2012;480:75-8.
13. Ekicibil A, Cetin SK, Ayaş AO, Coşkun A, Fırat T, Kıymac K. Exploration of the superconducting properties of $Y_3Ba_5Cu_8O_{18}$ with and without Ca doping by magnetic measurements. Solid State Sci. 2011;13(11):1954-9.
14. Naik SPK, Santosh M, Raju PMS. Structural and thermal validations of $Y_3Ba_5Cu_8O_{18}$ composites synthesized via citrate sol-gel spontaneous combustion method. J Supercond Nov Magn. 2017;31(5):1279-86.
15. Jongprateep O, Tangbuppa P, Manasnilobon N. Compositions and particle sizes of $(RE)Ba_2Cu_3O_{7-X}$ superconductor powders synthesized by the solution combustion technique. Adv Mat Res. 2012;488-489:286-90.
16. Saavedra I, Supelano G, Parra C. Determination of critical superconducting parameters based on the study of the magnetization fluctuations for $RE_3Ba_5Cu_8O_{18-\delta}$ (RE= Sm, Eu, Gd, Dy and Ho) ceramic superconductor system. Ceram Int. 2020;46(8):11530-8.
17. Topal U, Akdogan M. Further increase of T c in Y-Ba-Cu-O superconductors. J Supercond Nov Magn. 2011;24(5):1815-20.
18. Kutuk S, Bolat S. Levitation force of (RE)BCO-358 bulk superconductors. AIP Conference Proceedings. 2016;2042:020033.
19. Rivera AMM, Cuaspud JAG, Várgas CAP, Ramirez MHB. Synthesis and characterization of $LaBa_2Cu_3O_{7-\delta}$ system by combustion technique. J Supercond Nov Magn. 2016;29(5):1163-71.
20. Toby BH. EXPGUI, a graphical user interface for GSAS. J Appl Cryst. 2001;34(2):210-3.
21. Kraus W, Nolze G. POWDER CELL – a program for the representation and manipulation of crystal structures and calculation of the resulting X-ray powder patterns. J Appl Cryst. 1996;29(3):301-3.
22. Rekaby M, Awad R, Abou-Aly A, Yousry M. AC magnetic susceptibility of $Y_3Ba_5Cu_8O_{18}$ substituted by Nd^{3+} and Ca^{2+} ions. J Supercond Nov Magn. 2019;32(11):3483-94.
23. Pathak LC, Mishra SK. A review on the synthesis of Y–Ba–Cu-oxide powder. Supercond Sci Technol. 2005;18(9)
24. Supelano G, Santos AS, Vargas CP. Magnetic fluctuations on $TR_3Ba_5Cu_8O_8$ (TR=Ho, Y and Yb) superconducting system. Physica B. 2014;455:79-81.
25. Troć R, Bukowski Z, Horyń R, Klamut J. Possible antiferromagnetic ordering in $Y_2Cu_2O_5$. Paramagnetic behaviour of $BaCuO_2$. Phys Lett A. 1987;125(4):222-4.
26. Dias FT, Oliveira CP, Vieira VN, Silva DL, Mesquita F, Almeida ML, et al. Magnetic irreversibility and zero resistance in granular Y358 superconductor. J Phys Conf Ser. 2014;568(2):022009.
27. Rekaby M, Roumié M, Abou-Aly A, Awad R, Yousry M. Magnetoresistance study of $Y_3Ba_5Cu_8O_{18}$ superconducting phase substituted by Nd^{3+} and Ca^{2+} ions. J Supercond Nov Magn. 2014;27(10):2385-95.
28. Sumadiyasa M, Adnyana I, Wendri N, Suardana P. Journal of Materials Science and Chemical Engineering. 2017;5(11):44-53.